Cell Reports, Volume *35*

Supplemental information

Nanoscale 3D EM reconstructions reveal intrinsic mechanisms of structural diversity of chemical synapses

Yongchuan Zhu, Marco Uytiepo, Eric Bushong, Matthias Haberl, Elizabeth Beutter, Frederieke Scheiwe, Weiheng Zhang, Lyanne Chang, Danielle Luu, Brandon Chui, Mark Ellisman, and Anton Maximov

SUPPLEMENTAL INFORMATION

Supplemental figures and legends

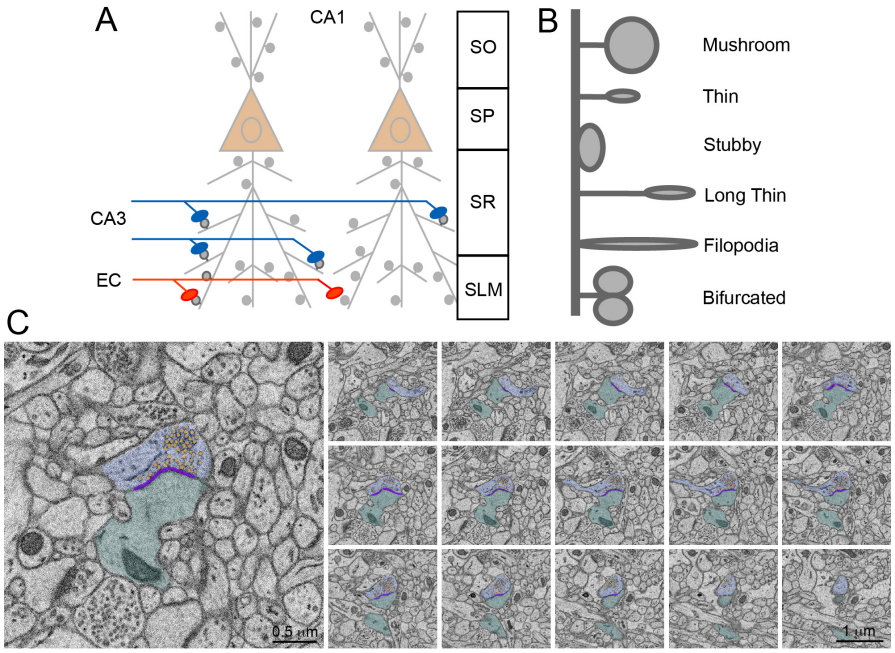

Figure S1. Related to Figure 1

(A) Schematics of excitatory circuits in the CA1. SO = Stratum oriens; SP = Pyramidal cell layer; SR = Stratum radiatum; SLM = Stratum lacunosum-moleculare; EC = entorhinal cortex. **(B)** Schematics of morphologically distinct spine types on PN dendrites. **(C)** 2D SBEM images in VAST with color-coded spines (green), postsynaptic densities (purple), presynaptic terminals (blue) and neurotransmitter vesicles (yellow). Scale bars are 0.5 and 1 µm (applies to all panels).

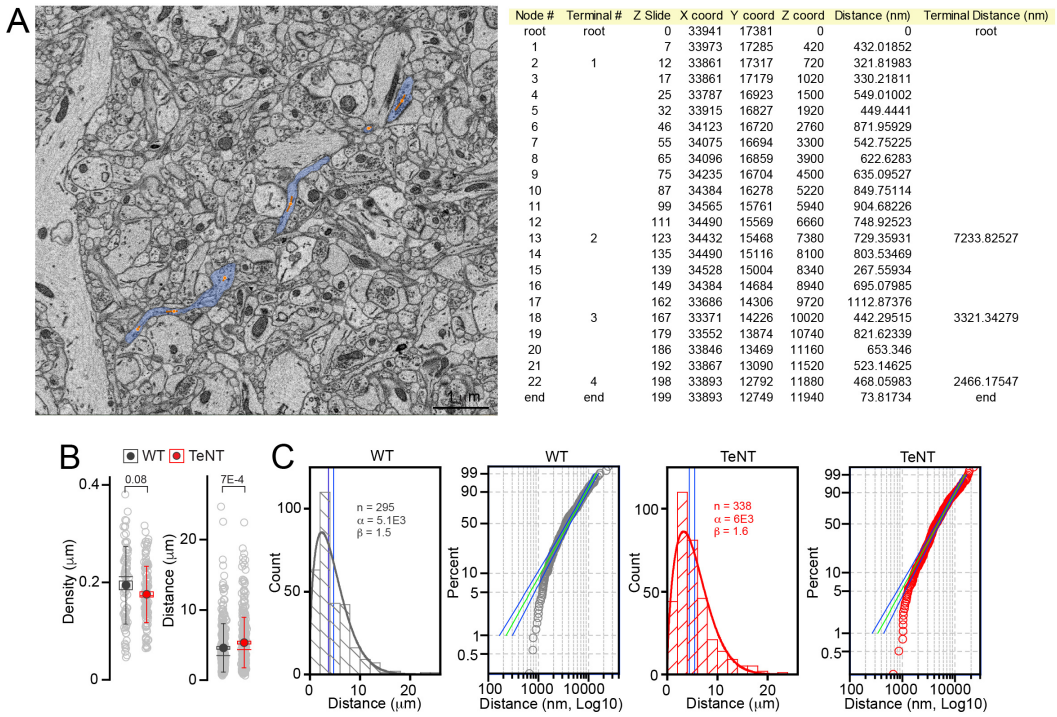

Node #	Terminal #	Z Slide	X coord	Y coord	Z coord	Distance (nm)	Terminal Distance (nm)
root	root	0	33941	17381	0	0	root
1		7	33973	17285	420	432.01852	
2	1	12	33861	17317	720	321.81983	
3		17	33861	17179	1020	330.21811	
4		25	33787	16923	1500	549.01002	
5		32	33915	16827	1920	449.4441	
6		46	34123	16720	2760	871.95929	
7		55	34075	16694	3300	542.75225	
8		65	34096	16859	3900	622.6283	
9		75	34235	16704	4500	635.09527	
10		87	34384	16278	5220	849.75114	
11		99	34565	15761	5940	904.68226	
12		111	34490	15569	6660	748.92523	
13	2	123	34432	15468	7380	729.35931	7233.82527
14		135	34490	15116	8100	803.53469	
15		139	34528	15004	8340	267.55934	
16		149	34384	14684	8940	695.07985	
17		162	33686	14306	9720	1112.87376	
18	3	167	33371	14226	10020	442.29515	3321.34279
19		179	33552	13874	10740	821.62339	
20		186	33846	13469	11160	653.346	
21		192	33867	13090	11520	523.14625	
22	4	198	33893	12792	11880	468.05983	2466.17547
end	end	199	33893	12749	11940	73.81734	end

Figure S2. Related to Figure 2

(A) Example of traced axons with annotated terminals and their 3D coordinates. Scale bar is 1 µm. **(B)** Densities of presynaptic terminals and distances between terminals along isolated axonal arbors in wildtype (WT) and *Emx1*$^{IRES\text{-}Cre}$/*R26*$^{floxstop\text{-}TeNT}$ mice (TeNT). Here and in all similar panels below, box with data overlap plots show raw data points (open grey circles), mean values (filled circles), standard errors (boxes), standard deviations (vertical lines) medians (horizontal lines) and p values, as defined by Mann-Whitney test. WT, n = 82 axons/295 terminals; TeNT, n = 121/338. **(C)** Spatial distributions of terminals along axonal shafts. Graphs show Weibull PDF curves generated by direct fitting of data (distances between boutons) without pre-binning, manually adjusted bins, vertical mean and median lines (blue), sample sizes (n = total numbers or presynaptic boutons), and distribution scales (α) and shapes (β). Probability plots accompanying distribution fits with reference (green) and 95% confidence (blue) lines are also shown in separate panels for each dataset. Note the differences in scales of X axes. Quantifications were performed using SBEM volumes from 2 WT and 3 TeNT mice.

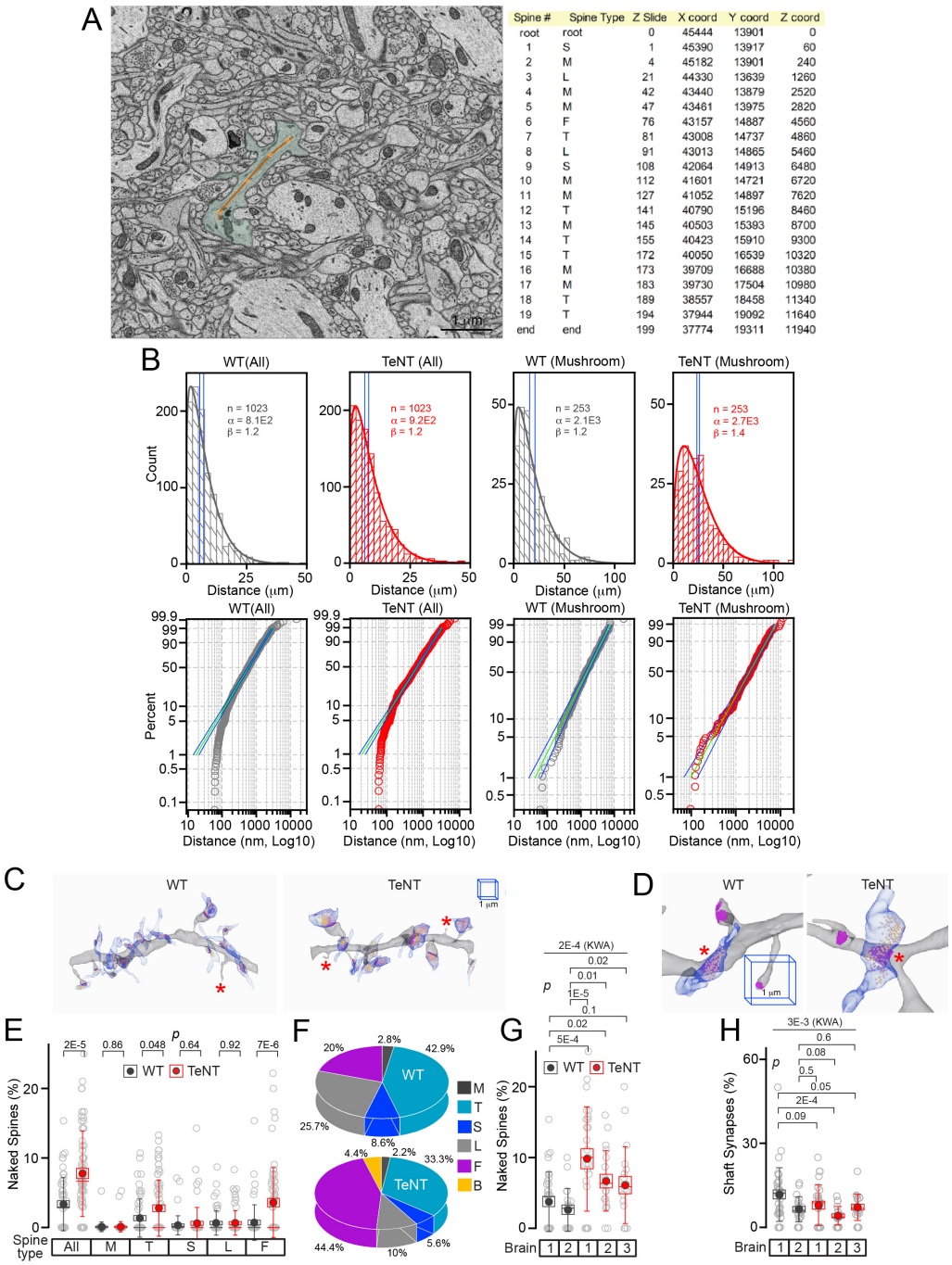

Figure S3. Related to Figure 2

(A) Example of traced dendrites with annotated spines and their 3D coordinates. Scale bar is 1 µm. **(B)** Spatial distributions of all and Mushroom-type innervated spines on PN dendrites in wildtype (WT) and *Emx1*$^{IRES\text{-}Cre}$/*R26*$^{floxstop\text{-}TeNT}$ mice (TeNT). Graphs show Weibull PDF curves generated by direct fitting of data (distances between spines), manually adjusted bins, vertical mean and median lines (blue), sample sizes (n = numbers or spines), and distribution scales (α) and shapes (β). Probability plots accompanying distribution fits with reference (green) and 95% confidence (blue) lines are also shown. **(C)** 3D reconstructions of dendritic branches with innervated and "naked" spines (asterisks). **(D)** 3D reconstructions of spineless synapses formed by Sc terminals onto dendritic shafts (asterisks). Scale bars apply to both panels. **(E** and **F)** Percentages (in E) and fractions (in F) of indicated types of "naked" spines on dendritic branches in mice of each genotype. WT (All), n = 55 branches; WT (M, T, S, L), n = 56; WT (F), n = 55; WT (B), n = 36. TeNT (All), n = 67; TeNT (M), n = 88; TeNT (T, S, L, F, B), n = 68. **(G** and **H)** Percentages of "naked" spines (in G) and synapses formed onto dendritic shafts (in H) in individual brains. WT Brain 1, n = 35 branches; WT Brain 2, n = 20; TeNT Brain 1, n=27; TeNT Brain 2, n=20; TeNT Brain 1, n=20.

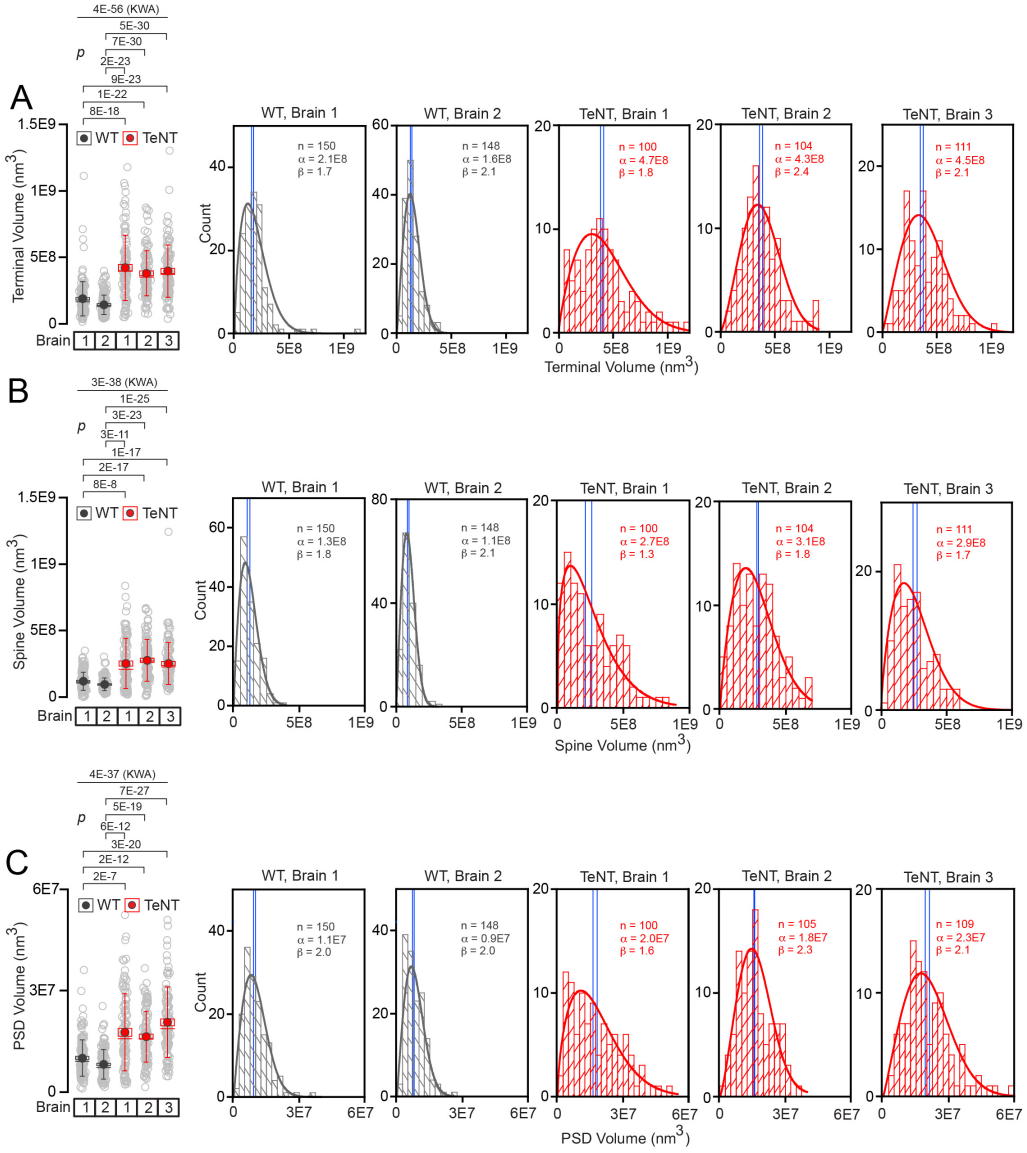

Figure S4. Related to Figure 3

Volumes of presynaptic terminals (in A), spines (in B) and PSDs (in C) of Mushroom-type synapses in individual brains of wildtype (WT) and *Emx1*$^{IRES\text{-}Cre}$/*R26*$^{floxstop\text{-}TeNT}$ mice (TeNT). p values were defined by Kruskal-Wallis ANOVA (top lines) followed by Mann-Whitney test. Sample sizes for terminals: WT Brain 1, n = 150; WT Brain 2, n = 148; TeNT Brain 1, n = 100; TeNT Brain 2, n = 104; TeNT Brain 3, n = 111. Sample sizes for spines: WT Brain 1, n = 150; WT Brain 2, n = 148; TeNT Brain 1, n = 100; TeNT Brain 2, n = 104; TeNT Brain 3, n = 111. Sample sizes for PSDs: WT Brain 1, n = 150; WT Brain 2, n = 148; TeNT Brain 1, n = 100; TeNT Brain 2, n = 105; TeNT Brain 3, n = 109. Weibull PDF plots show curves generated by direct fitting of data without pre-binning, manually adjusted bins, vertical mean and median lines (blue), sample sizes (n), and distribution scales (α) and shapes (β).

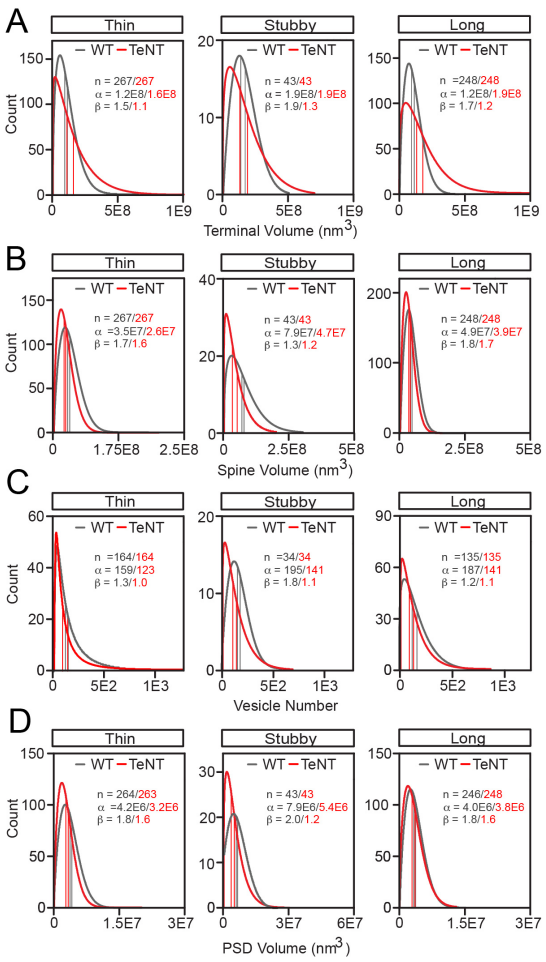

Figure S5. Related to Figure 3

Distributions of sizes of presynaptic terminals (in A), spines (in B), vesicle pools (in C) and PSDs (in D) in synapses formed onto Thin, Stubby and Long spines in wildtype (WT) and *Emx1*$^{IRES\text{-}Cre}$/*R26*$^{floxstop\text{-}TeNT}$ mice (TeNT). Graphs show Weibull PDF curves generated by direct fitting of data without pre-binning, vertical mean and median lines (color-coded), sample sizes (n), and distribution scales (α) and shapes (β). Quantifications were performed using SBEM volumes from 2 WT and 3 TeNT mice.

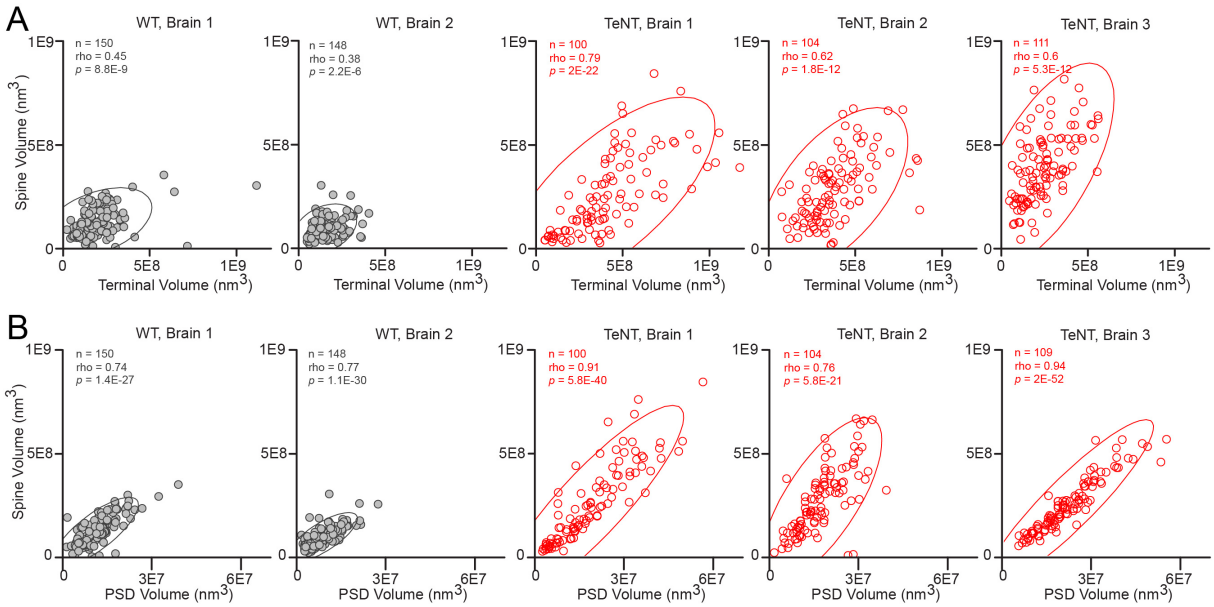

Figure S6. Related to Figure 4

Correlations between spine and terminal volumes (in A) and spine and PSD volumes (in B) in individual brains of wildtype (WT) and *Emx1*$^{IRES\text{-}Cre}$/*R26*$^{floxstop\text{-}TeNT}$ mice (TeNT). Scatter plots with confidence ellipses, sample sizes (n), Spearman correlation coefficients (rho), Fisher transformation scores (z) and p values are shown.

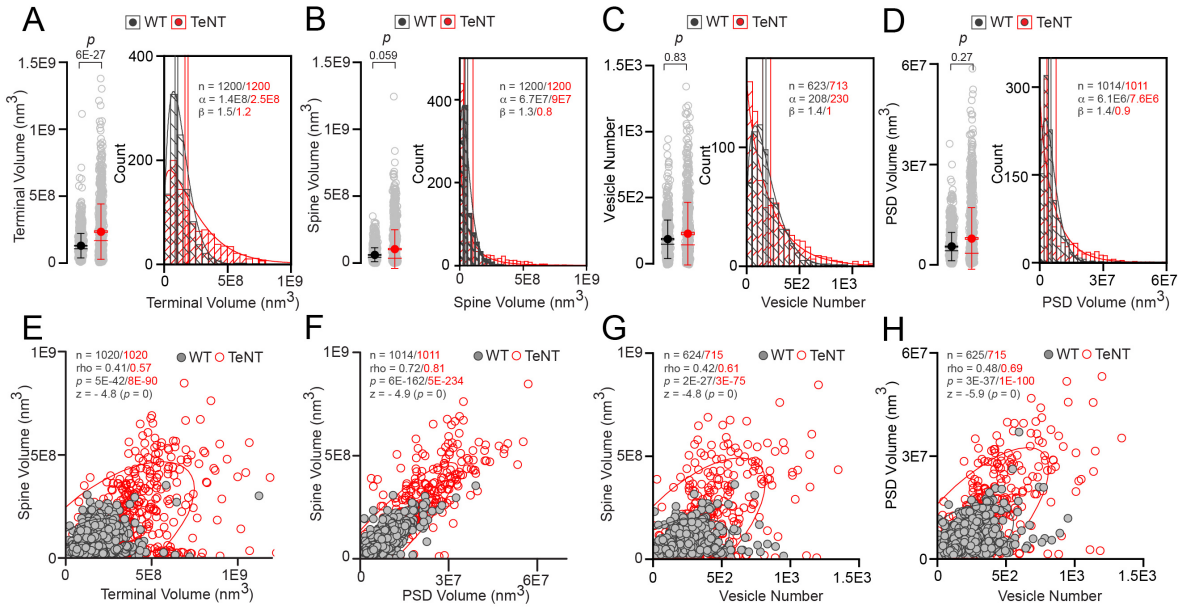

Figure S7. Related to Figures 3 and 4

"Generic" excitatory synapses were analyzed in the CA1sr of wildtype (WT) and *Emx1*$^{IRES\text{-}Cre}$/*R26*$^{floxstop\text{-}TeNT}$ mice (TeNT) without classification by spine type. **(A** to **C)** Box with data overlap and PDF plots show the distributions of terminal volumes (in A) spine volumes (in B) vesicle numbers (in C) and PSD volumes (in D). p values were defined by Mann-Whitney test. In PDF plots, sample sizes, curves generated by direct fitting of data without pre-binning, manually adjusted bins, vertical mean and median lines (color-coded) and distribution scales (α) and shapes (β) are shown. **(E** to **H)** Correlations between indicated pre- and postsynaptic parameters in individual units. Scatter plots with confidence ellipses, sample sizes (n), Spearman correlation coefficients (rho), Fisher transformation scores (z) and p values are shown. Quantifications were performed using SBEM volumes from 2 WT and 3 TeNT mice.

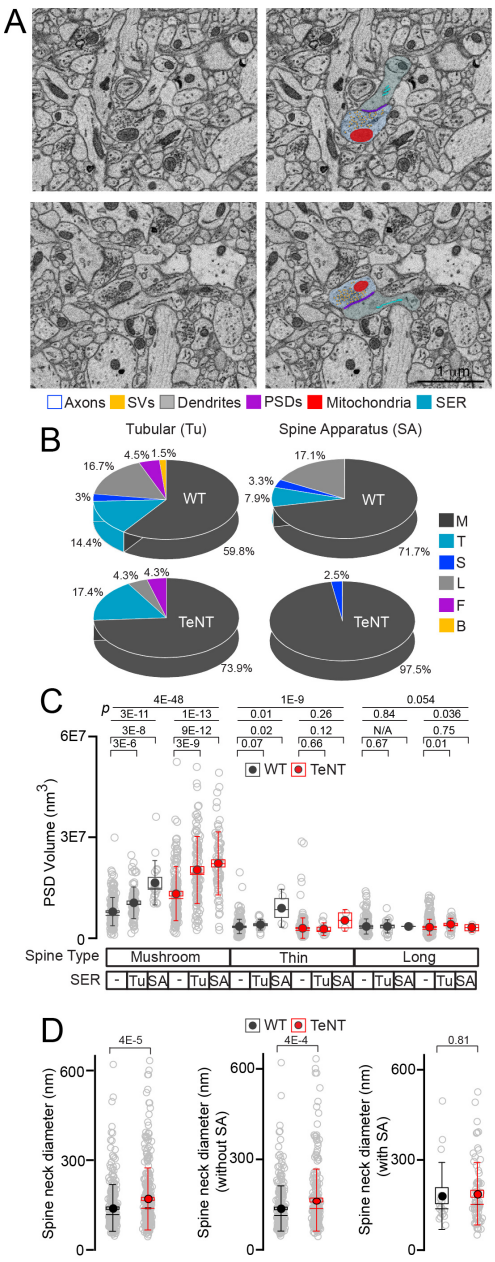

Figure S8. Related to Figure 6

(A) Examples of traced mitochondria and SER in SBEM volumes. Spines with Spine apparatus (top) and tubular SER (bottom) are shown. Scale bar is 1 µm (applies to all panels). **(B)** Fractions of indicated spine types with tubular SER (Tu) and spine apparatus (SA) in wildtype (WT) and *Emx1*$^{IRES\text{-}Cre}$/*R26*$^{floxstop\text{-}TeNT}$ mice (TeNT). WT (Tu), n = 132 spines; WT (SA), n = 32; TeNT (Tu), n = 152; TeNT (SA), n = 81. **(C)** Volumes of PSDs in indicated spine types with no smooth ER, with tubular ER, and with spine apparatus. WT (M, 0 - no SER), n = 211; WT (M, Tu), n = 77; WT (M, SA), n = 17; WT (T, 0), n = 265; WT (T, Tu), n = 19; WT (T, SA), n = 4; WT (L, 0). n = 233; WT (L, Tu), n = 22; WT (L, SA), n = 1; TeNT (M, 0), n = 135; TeNT (M, Tu), n = 108; TeNT (M, SA), n = 73; TeNT (T, 0), n = 258; TeNT (T, Tu), n = 12; TeNT (T, SA), n = 2; TeNT (L, 0), n = 271; TeNT (L, Tu), n = 26; TeNT (L, SA), n = 2. **(D)** Diameters of mushroom spine necks. Graphs show measurements in all spines and spines grouped into two categories based on the absence or presence of a spine apparatus (SA). WT (total), = 297; TeNT (total), n = 314; WT (no SA), n = 280; TeNT (no SA), n = 239; WT (SA), n = 17; TeNT (SA), n = 75. Quantifications were performed using SBEM volumes from 2 WT and 3 TeNT mice.